Supplementary Information:

Ribbon Aromaticity in Double-Chain Planar $B_nH_2^{2-}$ and $Li_2B_nH_2$ Nanoribbon Clusters Up to n = 22: Lithiumated Boron Dihydride Analogs of Polyenes

Hui Bai,[†] Qiang Chen,[†] Chang-Qing Miao,[‖] Yue-Wen Mu,[†] Yan-Bo Wu,[†]
Hai-Gang Lu,[†] Hua-Jin Zhai,*[,†] and Si-Dian Li*[,†]

[†] *Institute of Molecular Science, Shanxi University, Taiyuan 030006, People's Republic of China*

[‖] *Institute of Materials Science and Department of Chemistry, Xinzhou Teachers' University, Xinzhou 034000, Shanxi, People's Republic of China*

*E-mail: hj.zhai@sxu.edu.cn; lisidian@sxu.edu.cn

Complete ref 36.

Table S1. Calculated ADEs of $Li_2B_nH_2^-$ monoanions and IPs of $Li_2B_nH_2$ neutrals at PBE1PBE.

Figure S1. π CMOs of $Li_2B_nH_2^{0/-}$ (n = 6–12, 15, 16, 19, and 20) compared with those of C_4H_6, C_6H_8, C_8H_{10}, $C_{10}H_{12}$, and $C_{12}H_{14}$. Also shown are π CMOs of $B_{20}H_2^{2-}$.

Figure S2. σ CMOs of $Li_2B_nH_2^{0/-}$ (n = 6–12, 15, 16, 19, and 20) and $B_{20}H_2^{2-}$.

Figure S3. Computational ground-state adiabatic detachment energies (ADEs) of DC planar $B_nH_2^-$ (n = 4–20; empty squares) nanoribbon clusters as a function of n at the PBE1PBE/6-311+G(d,p) level, as compared with their experimental values (n = 7–12; solid squares). Also shown for comparison are theoretical ADEs of DC planar $B_n(BO)_2^-$ (n = 4–20; empty dots) nanoribbon clusters.

Complete ref 36.

(36) Gaussian 09, Revision A.1, Frisch, M. J.; Trucks, G. W.; Schlegel, H. B.; Scuseria, G. E.; Robb, M. A.; Cheeseman, J. R.; Scalmani, G.; Barone, V.; Mennucci, B.; Petersson, G. A.; Nakatsuji, H.; Caricato, M.; Li, X.; Hratchian, H. P.; Izmaylov, A. F.; Bloino, J.; Zheng, G.; Sonnenberg, J. L.; Hada, M.; Ehara, M.; Toyota, K.; Fukuda, R.; Hasegawa, J.; Ishida, M.; Nakajima, T.; Honda, Y.; Kitao, O.; Nakai, H.; Vreven, T.; Montgomery, Jr., J. A.; Peralta, J. E.; Ogliaro, F.; Bearpark, M.; Heyd, J. J.; Brothers, E.; Kudin, K. N.; Staroverov, V. N.; Kobayashi, R.; Normand, J.; Raghavachari, K.; Rendell, A.; Burant, J. C.; Iyengar, S. S.; Tomasi, J.; Cossi, M.; Rega, N.; Millam, J. M.; Klene, M.; Knox, J. E.; Cross, J. B.; Bakken, V.; Adamo, C.; Jaramillo, J.; Gomperts, R.; Stratmann, R. E.; Yazyev, O.; Austin, A. J.; Cammi, R.; Pomelli, C.; Ochterski, J. W.; Martin, R. L.; Morokuma, K.; Zakrzewski, V. G.; Voth, G. A.; Salvador, P.; Dannenberg, J. J.; Dapprich, S.; Daniels, A. D.; Farkas, Ö.; Foresman, J. B.; Ortiz, J. V.; Cioslowski, J.; Fox, D. J. Gaussian, Inc., Wallingford CT, 2009.

Table S1. Calculated ADEs of $Li_2B_nH_2^-$ monoanions and IPs of $Li_2B_nH_2$ neutrals at PBE1PBE.

species	ADE (eV)	IP (eV)
C_{2h} $Li_2B_6H_2^-$ (^2B_u)	0.67	
C_{2h} $Li_2B_6H_2$ (^1A_g)		6.06
C_{2v} $Li_2B_7H_2^-$ ($^1A_1$)	0.76	
C_{2v} $Li_2B_7H_2$ ($^2B_2$)		5.47
C_{2h} $Li_2B_8H_2^-$ (^2A)	0.86	
C_{2h} $Li_2B_8H_2$ (^1A_g)		5.69
C_{2v} $Li_2B_9H_2^-$ ($^1A_1$)	1.37	
C_{2v} $Li_2B_9H_2$ ($^2B_1$)		5.87
C_{2h} $Li_2B_{10}H_2^-$ (^2A_g)	1.01	
C_{2h} $Li_2B_{10}H_2$ (^1A_g)		6.16
C_{2v} $B_{11}H_2Li_2^-$ ($^1A_1$)	1.29	
C_{2v} $Li_2B_{11}H_2$ ($^2A_1$)		5.43
C_{2h} $Li_2B_{12}H_2^-$ (^2B_g)	1.65	
C_{2h} $Li_2B_{12}H_2$ (^1A_g)		5.57
C_{2v} $Li_2B_{13}H_2^-$ ($^1A_1$)	2.03	
C_{2v} $Li_2B_{13}H_2$ ($^2A_2$)		5.98
C_{2h} $Li_2B_{14}H_2^-$ (^2B_u)	1.43	
C_{2h} $Li_2B_{14}H_2$ (^1A_g)		6.16
C_{2v} $Li_2B_{15}H_2^-$ ($^1A_1$)	1.70	
C_{2v} $Li_2B_{15}H_2$ ($^2B_2$)		5.38
C_{2h} $Li_2B_{16}H_2^-$ (^2A_u)	2.21	
C_{2h} $Li_2B_{16}H_2$ (^1A_g)		5.50
C_{2v} $Li_2B_{17}H_2^-$ ($^1A_1$)	2.51	
C_{2v} $Li_2B_{17}H_2$ ($^2B_1$)		5.98
C_{2h} $Li_2B_{18}H_2^-$ (^2A_g)	1.80	
C_{2h} $Li_2B_{18}H_2$ (^1A_g)		6.04
C_{2v} $Li_2B_{19}H_2^-$ ($^1A_1$)	2.02	
C_{2v} $Li_2B_{19}H_2$ ($^2A_1$)		5.35
C_{2h} $Li_2B_{20}H_2^-$ (^2A_g)	2.48	
C_{2h} $Li_2B_{20}H_2$ (^1A_g)		5.59
C_{2v} $Li_2B_{21}H_2^-$ ($^1A_1$)	2.61	
C_{2v} $Li_2B_{21}H_2$ ($^1A_1$)		5.84
C_{2h} $Li_2B_{22}H_2^-$ (^2B_u)	2.10	
C_{2h} $Li_2B_{22}H_2$ (^1A_g)		5.85

Figure S1. π CMOs of $Li_2B_nH_2^{0/-}$ (n = 6–12, 15, 16, 19, and 20) compared with those of C_4H_6, C_6H_8, C_8H_{10}, $C_{10}H_{12}$, and $C_{12}H_{14}$. Also shown are π CMOs of $B_{20}H_2^{2-}$.

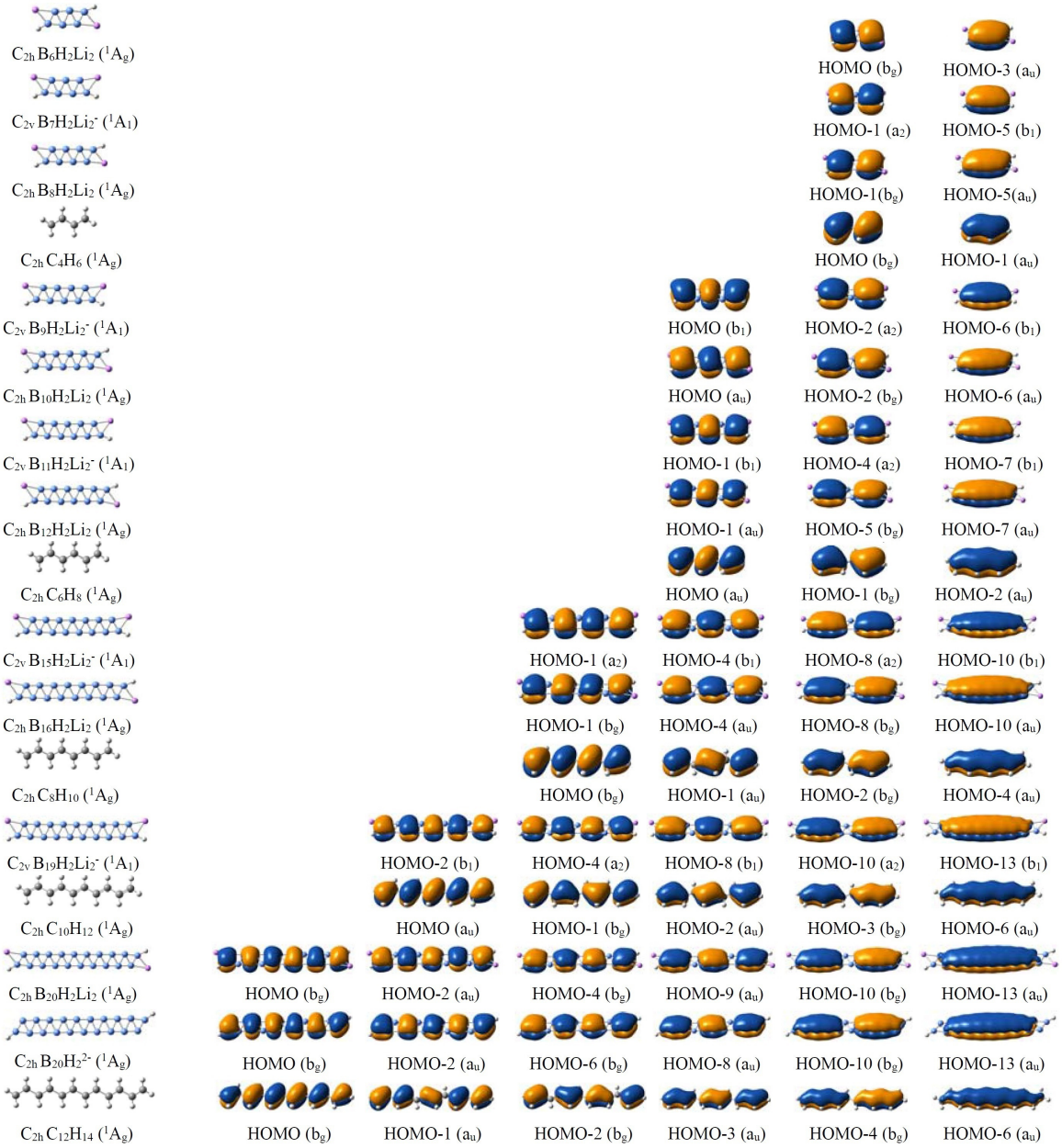

Figure S2. σ CMOs of $Li_2B_nH_2^{0/-}$ (n = 6–12, 15, 16, 19, and 20) and $B_{20}H_2^{2-}$.

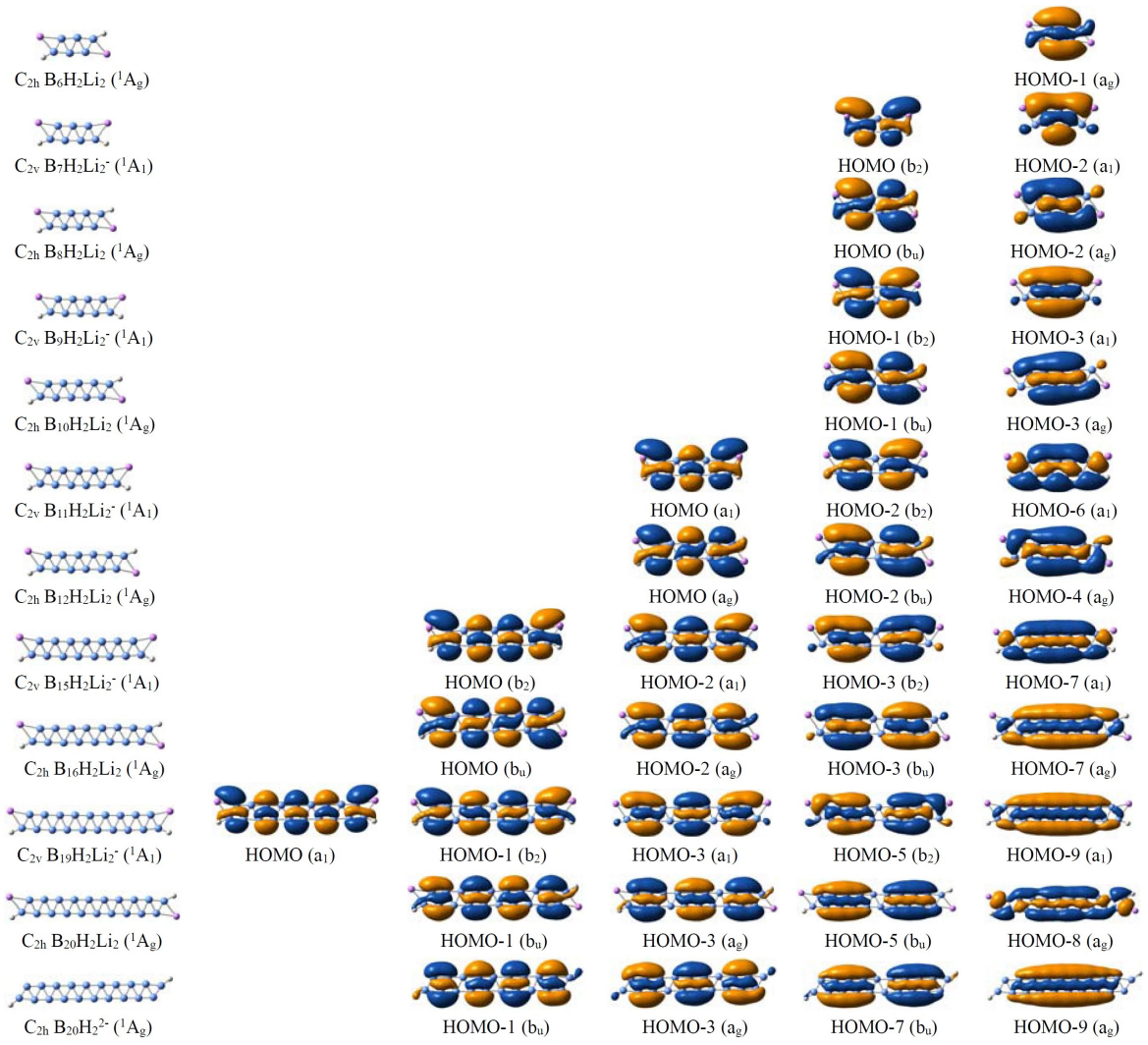

Figure S3. Computational ground-state adiabatic detachment energies (ADEs) of DC planar $B_nH_2^-$ (n = 4–20; empty squares) nanoribbon clusters as a function of n at the PBE1PBE/6-311+G(d,p) level, as compared with their experimental values (n = 7–12; solid squares). Also shown for comparison are theoretical ADEs of DC planar $B_n(BO)_2^-$ (n = 4–20; empty dots) nanoribbon clusters.